● RESEARCH ARTICLE

Combination of mild therapeutic hypothermia and adipose-derived stem cells for ischemic brain injury

Kai Zhao[1, #], Rui Li[2, #], Sheng Bi[3], Yu Li[1], Long Liu[1], Yu-Long Jia[1], Peng Han[1], Chang-Cong Gu[4], Xi-Ze Guo[4], Wan-Ping Zhang[4], Chun Wang[4], Chun-Ying Pei[4], Lin-Lu Tian[4], Li-Xian Li[1, *]

1 Department of Neurosurgery, First Affiliated Hospital of Harbin Medical University, Harbin, Heilongjiang Province, China
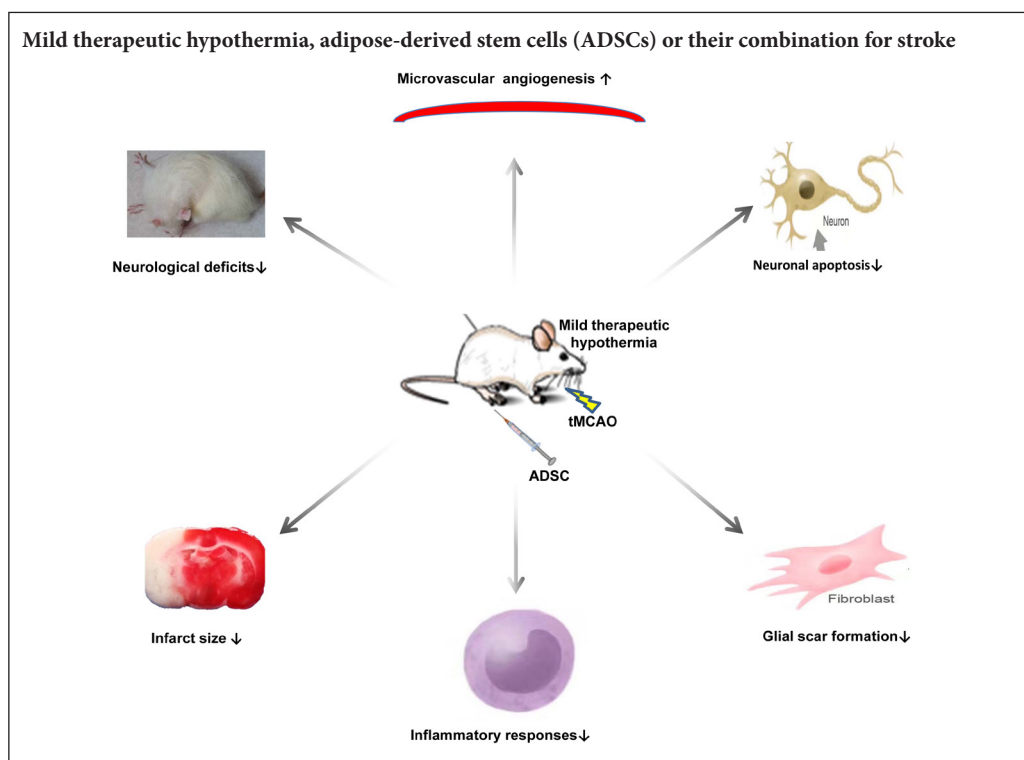2 Department of Neurology, University of Pennsylvania, Philadelphia, PA, USA
3 Department of Neurology, First Affiliated Hospital of Harbin Medical University, Harbin, Heilongjiang Province, China
4 Department of Immunology, Harbin Medical University, Harbin, Heilongjiang Province, China

Graphical Abstract

Mild therapeutic hypothermia, adipose-derived stem cells (ADSCs) or their combination for stroke

Microvascular angiogenesis ↑

Neurological deficits↓

Neuronal apoptosis↓

Mild therapeutic hypothermia

tMCAO

ADSC

Infarct size ↓

Glial scar formation↓

Inflammatory responses↓

Correspondence to:
Li-Xian Li, MD,
lilixian@hrbmu.edu.cn.

#These authors contributed
equally to this paper.

orcid:
0000-0003-4353-2229
(Li-Xian Li)

Abstract

Mild therapeutic hypothermia has been shown to mitigate cerebral ischemia, reduce cerebral edema, and improve the prognosis of patients with cerebral ischemia. Adipose-derived stem cell-based therapy can decrease neuronal death and infiltration of inflammatory cells, exerting a neuroprotective effect. We hypothesized that the combination of mild therapeutic hypothermia and adipose-derived stem cells would be neuroprotective for treatment of stroke. A rat model of transient middle cerebral artery occlusion was established using the nylon monofilament method. Mild therapeutic hypothermia (33°C) was induced after 2 hours of ischemia. Adipose-derived stem cells were administered through the femoral vein during reperfusion. The severity of neurological dysfunction was measured by a modified Neurological Severity Score Scaling System. The area of the infarct lesion was determined by 2,3,5-triphenyltetrazolium chloride staining. Apoptotic neurons were detected by terminal deoxynucleotidyl transferase-mediated dUTP-biotin nick end labeling (TUNEL) staining. The regeneration of microvessels and changes in the glial scar were detected by immunofluorescence staining. The inflammatory responses after ischemic brain injury were evaluated by *in situ* staining using markers of inflammatory cells. The expression of inflammatory cytokines was measured by reverse transcription-polymerase chain reaction. Compared with mild therapeutic hypothermia or adipose-derived stem cell treatment alone, their combination substantially improved neurological deficits and decreased infarct size. They synergistically reduced the number of TUNEL-positive cells and glial fibrillary acidic protein expression, increased vascular endothelial growth factor levels, effectively reduced inflammatory cell infiltration and down-regulated the mRNA expression of the proinflammatory cytokines interleukin-1β, tumor necrosis factor-α and interleukin-6. Our findings indicate that combined treatment is a better approach for treating stroke compared with mild therapeutic hypothermia or adipose-derived stem cells alone.

Key Words: nerve regeneration; brain injury; stroke; rats; transient middle cerebrum artery occlusion; cerebral resuscitation; mild therapeutic hypothermia; adipose-derived stem cells; combination therapy; neuroprotection; neuronal cell death; neural regeneration

Introduction

Stroke is one of the most common causes of disability and death worldwide (Hankey, 2013), and the global burden of stroke is continuously increasing. Current therapeutic approaches focus on removing blockage of a blood vessel by thrombolysis (such as tissue plasminogen activator) and surgery. However, these treatments usually have a small time window and have limited or no effect on neural regeneration, therefore they can only benefit 10% of patients (Fisher et al., 2015). There is a call for new therapies that can both limit ischemic brain injury and promote neural repair.

Increasing evidence suggests that mild therapeutic hypothermia (MTH) can increase the survival of patients suffering from ischemic insults such as stroke and cardiac arrest (Kammersgaard et al., 2002). Recently, various clinical trials have shown that hypothermia has promising neuroprotective effects against stroke. For patients with cerebral ischemia, hypothermia therapy includes local head cooling caps or helmet devices and intra-arterial cooling methods (Feigin et al., 2003). Compared with deep hypothermia ($\leq$ 30°C), mild hypothermia (between 30 and 33°C) has been shown to reduce brain injury resulting from focal or global cerebral ischemia with much stronger effect (Karibe et al., 1994; Zhao et al., 2007; Yenari et al., 2012). MTH improves the outcomes of resuscitation in rat models of cerebral ischemia reperfusion injury by reducing the metabolic rate of brain tissues, the area of infarct volume and edema, the inflammatory response, blood-brain barrier disruption, the release of cytotoxic substances, and neuronal apoptosis (Erecinska et al., 2003; Zhao et al., 2007; Yenari et al., 2012).

Mesenchymal stem cell (MSC)-based therapy is an emerging therapeutic approach for treating stroke. With more in-depth research, different injection routes have been used in the treatment of ischemic stroke, such as intracerebral (Chen et al., 2001a), intraventricular (Jin et al., 2005), intrastriatal (Li et al., 2000), and intra-arterial (Shen et al., 2006) alternatives. Each different injection route can improve behavior, so most researchers prefer the use of less invasive methods, such as intravenous administration. Stem cells including embryonic stem cells, hematopoietic stem cells, neural stem cells and MSCs are currently used to treat stroke (Chen et al., 2001b; Bacigaluppi et al., 2008; Li and Chopp, 2009). Of these cell types, MSCs are the most promising since they can be obtained from various tissues and have the capability of differentiating into mature cells, such as adipocytes, osteocytes and neural/glial cells. Bone marrow MSCs were the first reported to be used in the treatment of stroke. Compared with other MSCs, adipose-derived stem cells (ADSCs) have several unique advantages, including abundance, ease of accessibility, lack of ethical debate and low immunogenicity, and they may be the most abundant and interesting source for cell-replacement therapy (Zuk et al., 2001; Puissant et al., 2005; Tobita et al., 2011; Gao et al., 2014). We and others have shown that administration of MSCs from various origins substantially improves neurological deficits in animal models of stroke (Hao et al., 2014; Zhao et al., 2017). The potential mechanisms for the therapeutic effect of MSCs on stroke may involve secretion of neurotrophic factors that promote neural cell survival and growth (Leu et al., 2010; Jeon et al., 2013; Chi et al., 2016), enhancement of neurogenesis (Leu et al., 2010), angiogenesis (Leu et al., 2010; Nam et al., 2015), and modulation of neuroinflammatory responses (Lee et al., 2008; Leu et al., 2010).

Combination therapy is important for cerebral ischemia. It is suitable for the treatment of clinical patients and combined treatment is superior to monotherapies but the underlying mechanisms remain unknown. Several studies have shown that mild hypothermia combined either with neural stem cell transplantation or with hydrogen sulfide treatment can enhance functional recovery, reduce cerebral infarct volumes and decrease expression levels of inflammatory factors (Wang et al., 2014; Dai et al., 2016). However, there have been no reports about mild hypothermia combined with ADSCs for the treatment of ischemic stroke. In the present study, we explored the possibility of combining MTH and MSC-based therapy for treatment of acute stroke using the rodent transient middle cerebral artery occlusion (tMCAO) model.

Materials and Methods

Animals and experimental design

A total of 170 adult Sprague-Dawley rats were purchased from Liaoning Changsheng Biotechnology, Benxi, China [No. SCXK (Liao) 2010-0001], including 10 female rats and 160 male rats, with an average body weight range of 250–300 g. All rats were housed at room temperature with free access to food and water. Female rats were used for extraction and isolation of ADSCs. Middle cerebral artery occlusion (MCAO) was performed in male rats. All experimental procedures were approved by the Institutional Animal Care and Use Committee at Harbin Medical University in China (approval No. 2012010).

The male Sprague-Dawley rats were randomly assigned to five experimental groups (n = 32 in each group). In the sham group, the rats underwent surgery without infarct and received a saline solution in the femoral vein. In the vehicle group, the rats underwent surgery with tMCAO and received phosphate buffered saline (PBS) infusion in the femoral vein. In the ADSC group, the rats underwent tMCAO surgery and received an ADSC infusion in the femoral vein. In the MTH group, the rats underwent tMCAO surgery and MTH, without receiving an ADSC infusion. In the MTH + ADSC group, the rats underwent tMCAO surgery and MTH and received an ADSC infusion in the femoral vein. Details of the experimental protocol are shown in **Figure 1A**.

Isolation, characterization and transplantation of ADSCs

ADSCs were extracted from subcutaneous and abdominal adipose tissues of female Sprague-Dawley rats as previously described (Lee et al., 2009; Li et al., 2012). The extracted tissue was washed with sterile PBS and digested twice with 2% type I collagenase (Sigma-Aldrich, St. Louis, MO, USA) at 37°C for 60 minutes with shaking. Collagenase activity was neutralized with an equal volume of low-glucose Dulbecco's modified Eagle's medium (L-DMEM; Corning, Steuben

County, New York, USA) containing 10% fetal bovine serum (Corning). The filtered cells were centrifuged at 2000 r/min for 10 minutes to isolate the stromal vascular fraction. The cell pellets were filtered through a 70-μm pore size filter. Afterwards, cells were trypsinized and counted before being administered to the experimental animals. ADSCs (2×10^6 in 650 μL saline) were administrated through the femoral vein during reperfusion. Vehicle and sham-operated rats received a saline infusion only.

MSC surface markers detected by flow cytometry were used to validate the phenotype of ADSCs. Approximately 5×10^5 cells (100 μL of the cell suspension) were washed once with fluorescence activated cell sorting (FACS) buffer. The cells were then incubated with surface antibodies on ice for 20 minutes in the dark. After two washes, cells were acquired by flow cytometry (Accuri C6, BD). The fluorescently conjugated antibodies used for FACS were CD3-PE (555275, BD), CD19-FITC (561740, BD), CD31-PE (555027, BD), CD44-FITC (203906, Biolegend), CD45-FITC (202205, Biolegend), and CD90-APC (202507, Biolegend). The isotype controls were FITC-Mouse IgG2a, κ (400207, Biolegend), Alexa Fluor® 647-Mouse IgG1, κ (400130, Biolegend), and PE-Mouse IgG1, κ (550617, BD).

Differentiation of ADSCs *in vitro*
ADSCs were expanded in 35 mm culture plates (Corning) until passage 3, at 2×10^4 cells/cm².

Adipogenic differentiation: ADSCs were cultured for 14 days in an adipogenic induction medium, as previously described (Zeng et al., 2013). After 14 days of induction, the culture slides were stained with 2% fresh Oil Red-O solution (Sigma-Aldrich) for 5 minutes at room temperature to detect lipid droplets in the induced cells.

Osteogenic differentiation: ADSCs were induced for 28 days in an osteogenic induction medium, as previously described (Zeng et al., 2013). The culture medium was changed every 3 days. After 28 days of induction, the culture slides were stained with 5% silver nitrate solution under ultraviolet light for 1 hour.

Neural differentiation: 24 hours prior to neural induction, normal media were replaced with pre-induction media, as previously described (Safford et al., 2004). Cells were subjected to immunocytochemistry for neuronal nuclei (NeuN; 1:200; rabbit polyclonal antibody; Abcam, Cambridge, MA, USA) and Alexa Fluor-549-conjugated secondary antibody (1:400; Abcam). Images were acquired using a fluorescence microscope (Nikon, Tokyo, Japan).

tMCAO model establishment
The rats were intraperitoneally anesthetized with 10% chloral hydrate at a dose of 350 mg/kg. The rectal temperature was maintained at 37°C. Focal cerebral ischemia was induced by MCAO in rats as previously described (Longa et al., 1989; Chen et al., 2001b; Chiang et al., 2011). The left common carotid artery, external carotid artery and internal carotid artery of each rat were exposed *via* a midline neck incision. The tip of a 4-0 nylon monofilament was rounded

by heating over a flame and coated with silicone. To occlude the origin of the middle cerebral artery, the monofilament was moved carefully into the internal carotid artery lumen *via* the external carotid artery lumen until a slight resistance was felt. After 2 hours, the suture was slowly withdrawn to allow reperfusion. Intravenous injections of ADSCs (~2 $\times 10^6$) in 650 μL of PBS were administered for 5 minutes through the femoral vein after common carotid artery reperfusion. Poor activity of the right limbs of the rat indicated the success of the model surgery.

Induction of MTH
During the 2 hours of ischemia the rats were placed in a stereotaxic apparatus. The skull was drilled at 2.0 mm lateral to the bregma and implanted with a brain temperature probe (Thermometer, Taiwan, China; No. 2013082512) with its temperature sensor inserted approximately 4 mm from the skull surface. For hypothermia treatment, the rats were individually kept under cold conditions (4°C) and the individual cortical temperature was continuously maintained at 33 ± 1°C. Simultaneously, the anal temperature was controlled at 37 ± 1°C, as shown in **Figure 1B**.

In vitro experiments
Oxygen-glucose deprivation (OGD), ADSC treatment, and cell viability assays
To study whether ADSCs can play a neuroprotective role *in vitro* as well as *in vivo*, to model ischemia *in vitro*, cultured neuroblastoma cells (SH-SY5Y, Chinese Academy of Sciences, China) were exposed to OGD. On day 1, cells were plated at a density of 4×10^3 cells/well in 96-well plates and grown for 24 hours in F12/DMEM (Corning) supplemented with 10% fetal bovine serum (Gibco, Carlsbad, CA, USA) and 1% penicillin-streptomycin at 37°C in 5% CO_2/95% air. On the second day, the media were replaced by media mixed with ADSC supernatant: ADSC supernatant was added and the cells were induced by OGD for 24 hours at 33°C or 37°C in a humidified hypoxia chamber. L-DMEM was used as a control. Cell viability and cytotoxicity were quantified with 3-(4,5-dimethylthiazol-2-yl)-2,5-diphenyl tetrazolium bromide (MTT) and lactate dehydrogenase assays, respectively. All *in vitro* ischemia experiments were conducted in triplicate. A total of 15 wells were used for normal, 21 wells for OGD at 37°C, 21 wells for OGD at 33°C, and 15 wells for ADSC supernatant under OGD at 37°C, and 15 wells for ADSC supernatant under OGD at 33°C. Absorbance was measured at 450 nm (MTT assay, 4-hour incubation) or 490 nm (lactate dehydrogenase assay, 60-minute incubation) using a SpectraMax190 instrument (Molecular Devices).

In vivo experiments
Functional evaluation scale
All rats were neurologically evaluated at 1 and 7 days with the modified Neurological Severity Score Scaling System (Chen et al., 2005) by two researchers who were blinded to the experimental groups. The modified Neurological Severity Score was defined as follows: raising the rat by the tail (3),

placing the rat on the floor (normal = 0 and maximum = 3), sensory test (2), beam balance test (normal = 0 and maximum = 6), reflexes absent and abnormal movements (4). In all, a score of 1–6 indicated mild injury, 7–12 moderate injury, and 13–18 severe injury.

Measurement of lesion size by 2,3,5-triphenyltetrazolium chloride (TTC) staining

On days 1 and 7 after transplantation of ADSCs, rats were anesthetized with 10% chloral hydrate and transcardially perfused with saline. The brain tissues were rapidly removed, sliced into seven 2-mm-thick coronal sections and stained with 1% TTC solution at 37°C for 10 minutes. The stained slides were washed in PBS for 5 minutes and immersed overnight in 4% paraformaldehyde. The areas unstained by TTC were identified as the areas of infarction. The infarction volume was presented as a percentage of the volume of the contralateral hemisphere. ImageJ software (National Institutes of Health, Bethesda, MD, USA) was used to analyze the percentage of TTC stained tissue with respect to the whole piece of tissue.

Immunohistochemistry

Paraffin sections (5-μm-thick) were obtained from rats 24 hours after reperfusion. Microglial activation was measured using Iba1 expression. The sections were initially incubated with 3% hydrogen peroxide for 10 minutes, and then blocked for 1 hour. Rabbit polyclonal anti-Iba1 antibody (microglia marker, diluted 1:400; Abcam) at 4°C overnight was used as the primary antibody. Goat anti-rabbit IgG Biotin (1:60) at 37°C for 30 minutes was used as the secondary antibody. Anti-rabbit horseradish peroxidase (1:60) was added for 30 minutes at room temperature. Finally, nuclei were stained with hematoxylin. Counting of the immunopositive cells in each area was performed using a 20× objective and image analysis software (ImageJ) and calculated as counts per square millimeter by a single blinded investigator who had no knowledge of the assignment of treatment groups, as previously described (Yu et al., 2016).

Immunofluorescence

Frozen sections (5-μm-thick) were obtained from rats at 24 hours. The peri-infarct area was analyzed in brain sections using various antibodies to mark: neuronal nuclei (NeuN; neurons, rabbit polyclonal antibody diluted 1:100; Abcam), glial fibrillary acid protein (GFAP, astrocytes, rabbit polyclonal antibody diluted 1:400; Abcam), vascular endothelial growth factor (VEGF, rabbit polyclonal antibody diluted 1:200; Abcam), myeloperoxidase-carboxy terminal end (MPO; neutrophils, rabbit polyclonal antibody diluted 1:100; Abcam). After washing with PBS, sections were incubated with an Alexa Fluor 549-conjugated secondary antibody (diluted 1:400; Abcam), and nuclei were stained with 4,6-di-amidino-2-phenylindole (Beyotime Institute of Biotechnology, Shanghai, China). Six consecutive slices were subjected to immunofluorescence staining. Images were acquired using a fluorescence microscope (Nikon).

Terminal deoxynucleotidyl transferase-mediated dUTP-biotin nick end labeling (TUNEL) assay

TUNEL was used to identify apoptotic cells, particularly neurons, with nuclear DNA fragmentation in ischemic areas of the brain. The entire process was performed according to the manufacturer's instructions (Cat#11684809910, Roche). After fixation (4% paraformaldehyde in PBS, pH 7.4) for 20 minutes, samples were incubated in permeabilization solution (0.1% Triton X-100 in 0.1% sodium citrate, freshly prepared) for 2 minutes on ice. TUNEL reaction mixture (Enzyme solution and Label solution (1:10)) was added and incubated for 60 minutes at 37°C in a humidified atmosphere in the dark. Positive cells were counted as previously described (Yu et al., 2016).

RNA isolation and quantitative real-time reverse transcription-polymerase chain reaction (RT-PCR)

Brains were obtained from rats at 24 hours. Total RNA was isolated from the ischemic cortex using TRIzol reagent (Invitrogen) according to the manufacturer's instructions and reverse-transcribed into cDNA (Roche). Quantitative real-time RT-PCR was performed using SYBR-Green (Roche). The genes of the measured cytokines were amplified using the primers listed in **Table 1**.

Enzyme linked immunosorbent assay (ELISA) assay

Blood was obtained from each rat at 24 hours. VEGF protein levels in serum were measured by a commercial magnetic bead-based Multiplex ELISA kit (Elabscience) according to the manufacture's protocol. Samples were allowed to clot for 2 hours before centrifugation for 20 minutes at approxi-

Table 1 Primers used in real-time polymerase chain reaction

| Gene	Sequence (5′–3′)	Product size (bp)
Interleukin-1β	Forward: CTG TCC CTG AAC TCA ACT GTG	222
	Reverse: GTC CTC ATC CTG GAA GCT CC	
Tumor necrosis factor-α	Forward: GAT CGG TCC CAA CAA GGA GG	275
	Reverse: GCT GGT ACC ACC AGT TGG TTG	
Interleukin-6	Forward: CAG GGA GAT CTT GGA AAT GAG	300
	Reverse: GTT GTT CTT CAC AAA CTC C	
Chitinase3-like3 (Ym1)	Forward: GCG GAC CTA TGG CTT TGA TG	304
	Reverse: GCA GCA CTG AGC AGG AGT TTC	
Vascular endothelial growth factor	Forward: CAC CCA CGA CAG AAG G	385
	Reverse: TCA CAG TGA ACG CTC C	
β-Actin	Forward: ACG TTG ACA TCC GTA AAG AC	603
	Reverse: GAA GGT GGA CAG TGA GGC	
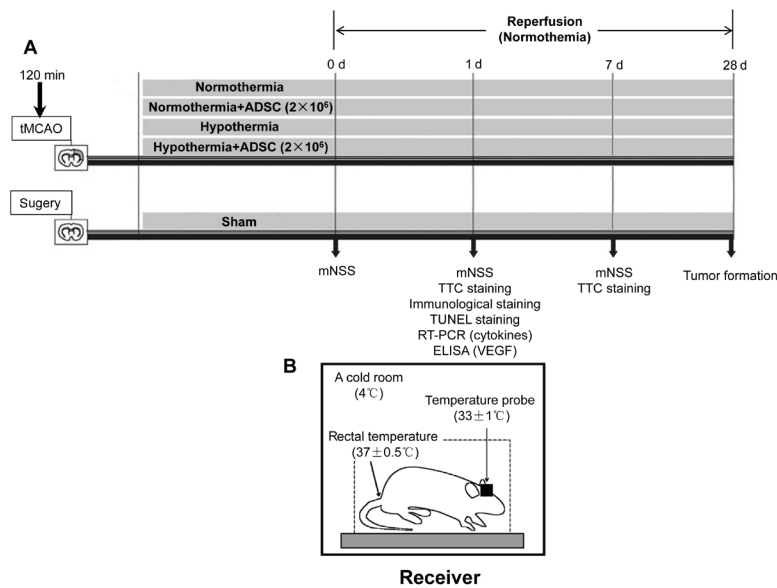
Figure 1 Therapeutic protocol and experimental design.
(A) Rats were randomly divided into five different groups: sham, vehicle (normothermia + saline), MTH (hypothermia + saline), ADSC group (normothermia + ADSCs), MTH + ADSC (hypothermia + ADSCs). Two-hour hypothermia was performed before the administration of ADSCs. A modified Neurological Severity Score Scaling System was performed on days 0, 1 and 7 and 2,3,5-triphenyltetrazolium chloride staining was performed on day 1 and day 7. Tumor formation was determined on day 28. (B) Induction of MTH. MTH: Mild therapeutic hypothermia; ADSC: adipose-derived stem cell; d: day(s).

mately $1000 \times g$. The serum was incubated in the wells for 2 hours at room temperature. After three washes, the samples were incubated for 2 hours with the concentrated biotinylated detection antibody. Finally, the samples were incubated for 20 minutes in streptavidin-horseradish peroxidase and in substrate solution (1:1 mixture of Color Reagent A (H_2O_2) and Color Reagent B (Tetramethylbenzidine) for 20 minutes. The development was finished with HCl and the protein content was determined at 450 nm using a SpectraMax190 instrument (Molecular Devices).

Tumor formation
Cardiac perfusion was performed on day 28 after treatment. Paraffin sections (5-μm-thick) of the spinal cord, lung, liver, spleen, kidney, bowel and lymph were analyzed. Moreover, tumor formation and the presence of infiltrating cells were analyzed in the peripheral organs at 28 days after ADSC administration using hematoxylin-eosin staining; no differences were observed when comparing vehicle and ADSC groups and no tumor formation was observed, demonstrating the safety of this treatment. Images were captured using an electron microscope (Nikon).

Statistical analysis
Data were represented as the mean ± SEM and analyzed using GraphPad Prism 6 software (GraphPad Software Inc., San Diego, CA, USA). All statistical analyses were performed using one-way analysis of variance followed by a Tukey's *post hoc* test for multiple comparisons. A P value < 0.05 was considered statistically significant.

Results
ADSC characterization and differentiation potential
ADSCs were isolated from adipose tissue surrounding subcutaneous and abdominal tissue. To characterize the phenotype of ADSCs, cells were stained with both positive and negative markers for ADSCs. These markers were detected by flow cytometry (**Figure 2A**). With our ADSC isolation and purification system we achieved more than 95% purity, as indicated by CD44 and CD90 positive cells (**Figure 2A**). Isolated ADSCs produced typical sphere-like colonies, with fibroblastic morphology (**Figure 2B**). To test the differentiation potential of these cells, ADSC differentiation was induced in three different directions: toward adipocytes, osteoblasts, and neural cells. After adipogenic induction, the cells were round and polygonal, with cytoplasm that contained many bright, highly refractive lipid droplets. Oil red-O staining further demonstrated the presence of lipid droplets after adipogenic differentiation (**Figure 2C**). Osteogenic induction of ADSCs was demonstrated by Von Kossa staining, which showed calcified extracellular matrix and confirmed ADSCs could differentiate into osteogenic cells (**Figure 2D**). After neural induction, the majority of cells were positive for the neuronal marker, NeuN (**Figure 2E**).

MTH in combination with ADSCs improved functional recovery and reduces infarct size after tMCAO
To test whether the combination of MTH and ADSCs could further benefit neural function recovery after tMCAO, we induced tMCAO in rats and a 2-hour local MTH treatment was applied before ADSC administration. Neurological behavior was independently evaluated at 1 and 7 days by two researchers who were blinded to the experimental groups (**Figure 3A** and **B**). TTC staining was used to measure the size of ischemic area (**Figure 3C–F**). Consistent with previous observations (Lee et al., 2016; Zhao et al., 2017), treatment with MTH or ADSCs alone improved neurological deficits and reduced the size of the infarct area. Interestingly, compared with single treatments, the combination of MTH and ADSC treatment further improved neural function recovery and decreased the ischemic lesion size (**Figure 3**). We did not observe any tumor formation in the major organs, including spinal cord, lung, liver, spleen, kidney, and intestine up to 28 days after the combination treatment (**Figure**
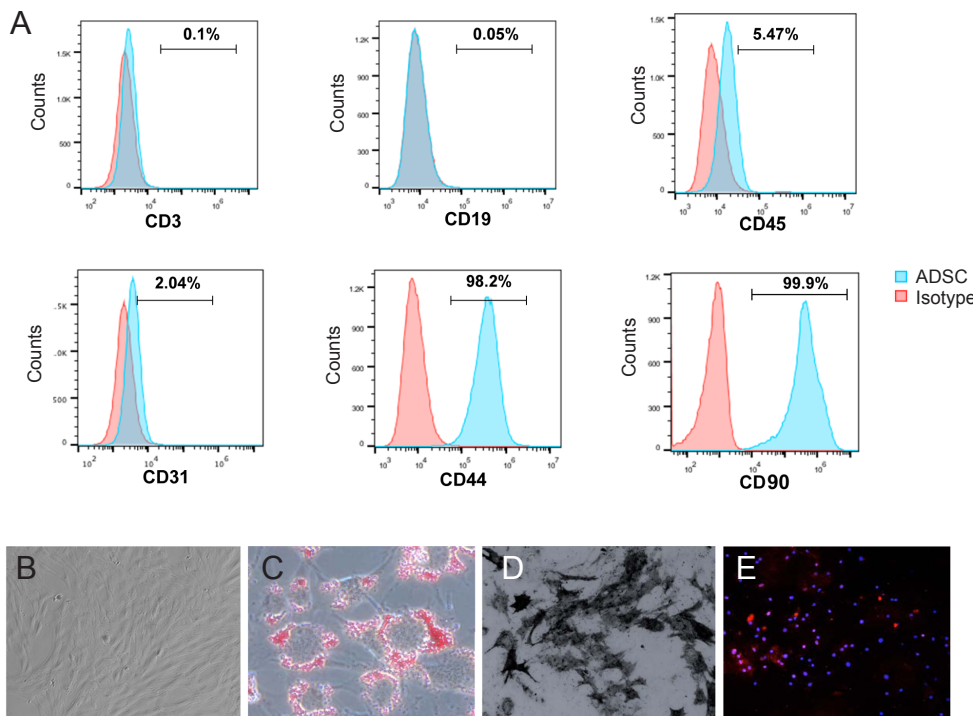
Figure 2 Adipose-derived stem cell (ADSC) characterization and differentiation potential.
(A) Flow cytometric analysis was used to measure surface markers of ADSCs. In our current culture protocol, we achieved more than 95% ADSC purity. (B) ADSCs showed a spindle-shaped, fibroblastic morphology under an electron microscope. (C) After adipogenic induction, the cells became round and polygonal, with cytoplasm that contained a large number of Oil red+ lipid droplets by Oil red staining. (D) After osteogenic induction, calcified extracellular matrix was identified by Von Kossa staining. (E) Immunofluorescence staining after neural induction: cells were positive for the neuronal marker NeuN. Orginal magnification: 20× in B, C, E, 40× in D.
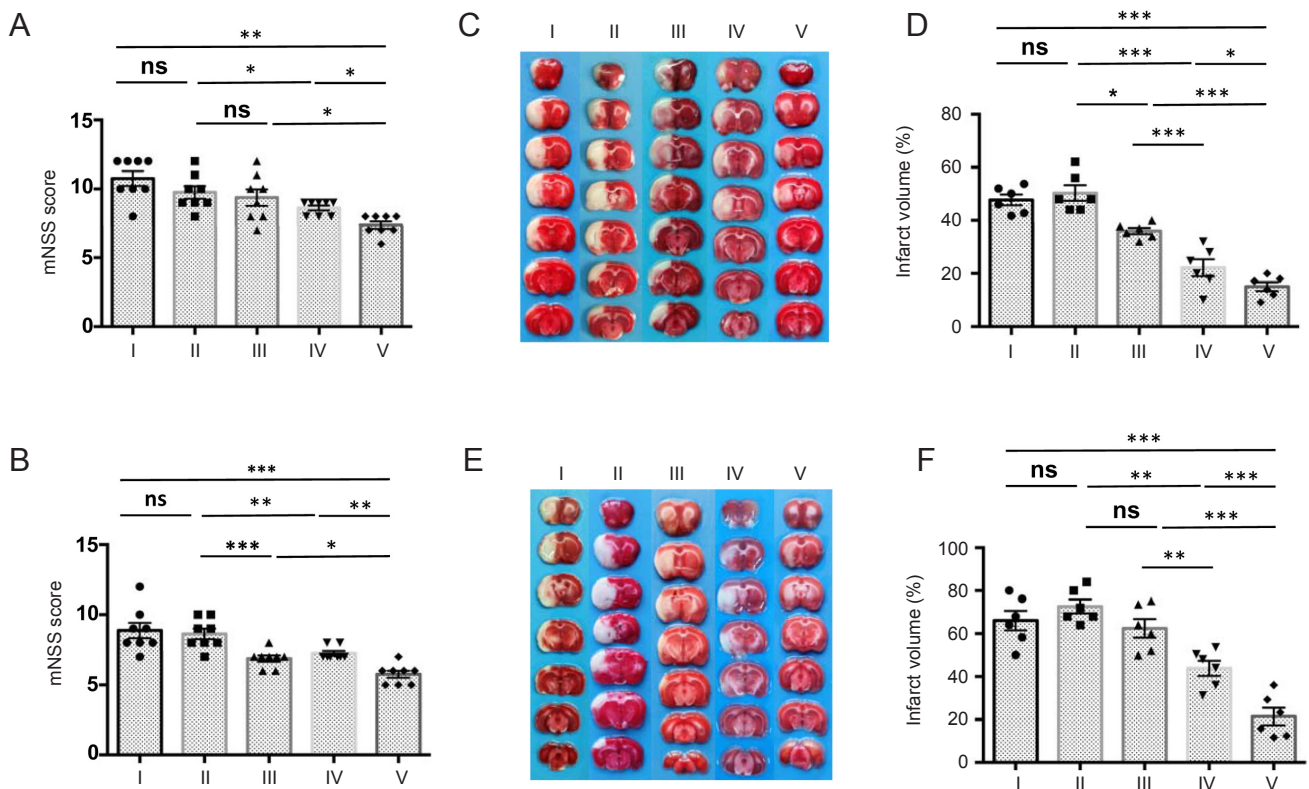
Figure 3 MTH in combination with ADSCs improved functional recovery and reduces infarct size after transient middle cerebral artery occlusion.
Neurological deficits were evaluated by a modified Neurological Severity Score on (mNSS) day 1 (A) and day 7 (B) by two independent researchers who were blinded to the experimental groups (n = 8 per group). The size of the infarct lesion was measured by 2,3,5-triphenyltetrazolium chloride staining on day 1 (C and D) and day 7 (E and F) (n = 6 per group; white indicates infarct region). Compared with single treatments, the combination of MTH and ADSCs further improved neurological function and decreased the ischemic lesion. All data are shown as the mean ± SEM ($*P$ < 0.05, $**P$ < 0.01, $***P$ < 0.001; one-way analysis of variance followed by a Tukey's *post hoc* analysis). I: Sham group; II: vehicle group (MCAO + PBS); III: ADSC group (MCAO + ADSC); IV: MTH group (MCAO + MTH); V: MTH + ADSC group (MCAO + MTH + ADSC). MTH: Mild therapeutic hypothermia; ADSC: adipose-derived stem cell; ns: not significant.
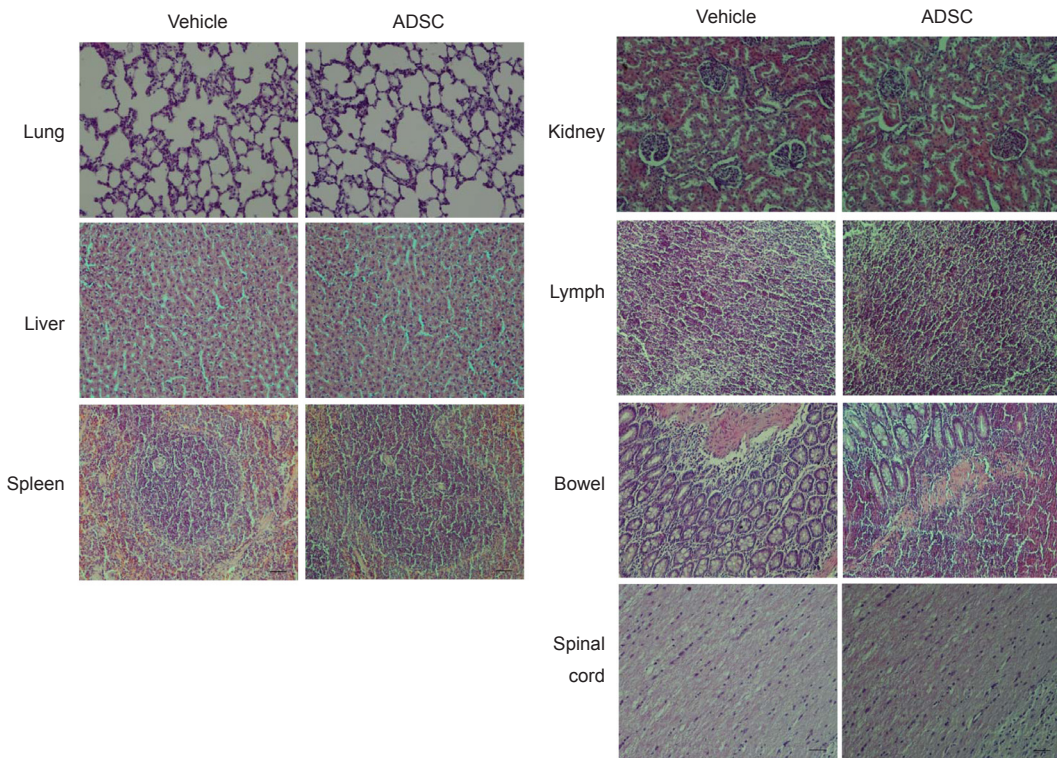
Figure 4 Effects of mild therapeutic hypothermia combined with adipose-derived stem cells on tumor formation.
Tumor formation was analyzed in various major organs at 28 days using hematoxylin-eosin staining. No tumor formation was observed. Original magnification, 20×. Scale bars: 100 μm. ADSC: Adipose-derived stem cell.
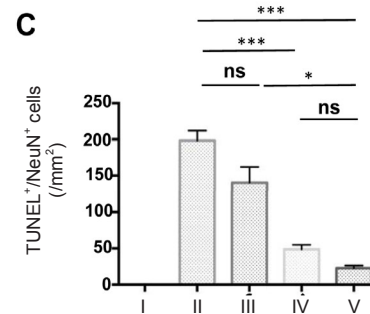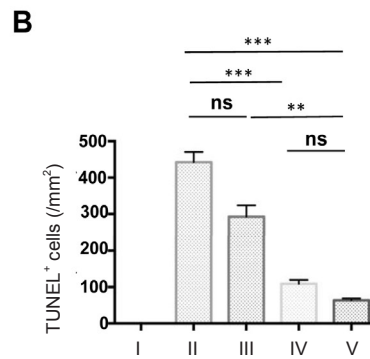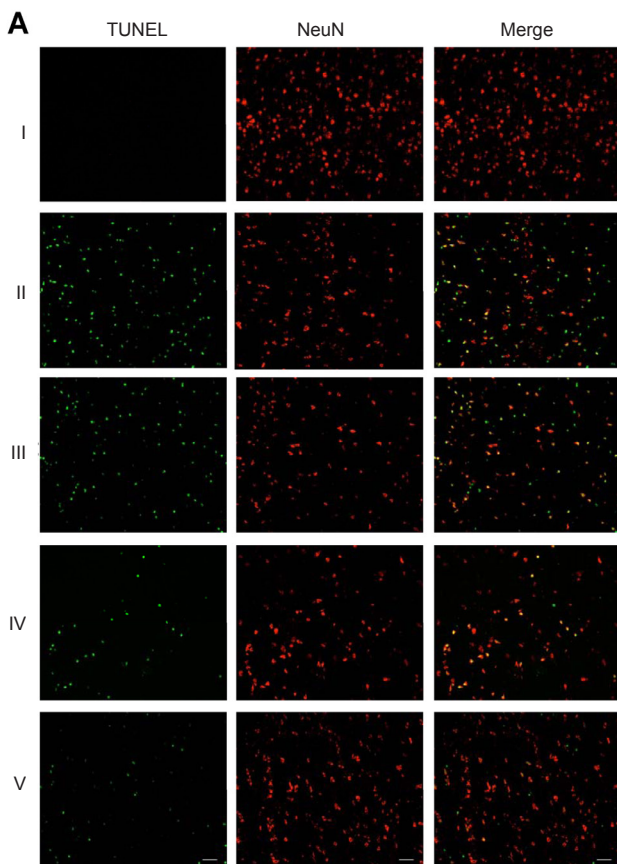

Figure 5 MTH in combination with ADSC administration dramatically reduces neuronal apoptosis *in vivo*.
(A) Images of colocalization of TUNEL and NeuN in the ischemic core of the cerebral cortex; Green: TUNEL, Red: NeuN. Scale bars: 100 μm. (B) Counts of TUNEL-positive cells. (C) Counts of TUNEL/NeuN-positive cells. Results are presented as the mean ± SEM ($n = 6$ per group; one-way analysis of variance followed by a Tukey's *post hoc* analysis); *$P < 0.05$, **$P < 0.01$, ***$P < 0.001$. I: Sham group; II: vehicle group (MCAO + PBS); III: ADSC group (MCAO + ADSC); IV: MTH group (MCAO + MTH); V: MTH + ADSC group (MCAO + MTH + ADSC). MTH: Mild therapeutic hypothermia; ADSC: adipose-derived stem cell; TUNEL: terminal deoxynucleotidyl transferase-mediated dUTP-biotin nick end labeling; NeuN: neuronal nuclei; ns: not significant.

4). Together, these data suggested that MTH combined with ADSC treatment is a safe approach that can further improve functional recovery and reduce infarct size at both early and late stages.

MTH in combination with ADSC administration reduced neuronal apoptosis *in vivo*

In a typical lesion of ischemic stroke, neurons within the core area usually rapidly become necrotic, while in the penumbral area surrounding the necrotic core, many neurons undergo apoptosis after several hours or days (Zhao et al., 2017). How to rescue these pre-apoptotic neurons in the penumbra from apoptosis is one of the main focuses in the field. Thus, we tested whether the combination of MTH and ADSCs could save neurons in this area. Late apoptotic neurons were identified by using TUNEL together with NeuN staining. The combination therapy substantially limited the number of TUNEL-positive neurons within the penumbra (**Figure 5A–C**).

MTH increased the responsiveness of ischemic neurons to ADSC treatment *in vitro*

The observation above indicates a potential additive therapeutic effect of the combination strategy. One of the possibilities is that MTH may increase the responsiveness of ischemic neurons to ADSC treatment. To test this possibility, SH-SY5Y cells were cultured under OGD conditions. The cells were cultured at the normal 37°C or at 33°C for 24 hours. Cell culture supernatants collected from ADSCs was added to the cells (**Figure 6A**). Relative cell viability and death were determined by MTT and lactate dehydrogenase assays, respectively. SH-SY5Y cells treated with MTH and ADSC supernatant showed increased viability (**Figure 6B**) and decreased cytotoxicity (**Figure 6C**) compared with single treatments. These results together indicated that MTH may increase the responsiveness of ischemic neurons to ADSC treatment.

MTH in combination with ADSC administration reduced astrogliosis and promoted angiogenesis

Astrogliosis refers to an increase in the number of astrocytes surrounding injured neurons, and has been observed in many neurological conditions, including stroke (Sofroniew et al., 2005). Astrogliosis is one of the initial steps in the formation of the glial scar (Gutiérrez-Fernández et al., 2015). Despite the ability of the glial scar to limit the spread of neural injury, glial scars create a physical barrier that strongly inhibits neural regeneration (Sofroniew et al., 2005). To measure whether the combination of MTH and ADSCs has an effect on astrogliosis, the number of astrocytes was compared among the different groups using the astrocyte marker, GFAP. The combination of MTH and ADSCs strongly decreased the number of GFAP$^+$ astrocytes compared with MTH or ADSC treatment alone (**Figure 7A–C**).

Angiogenesis after ischemic neural injury nourishes both injured and newly differentiated neurons, and therefore plays a crucial role in promoting neuron survival and neu-

ral regeneration (Gutiérrez-Fernández et al., 2011, 2015). Here, the expression of VEGF was used as a biomarker to determine the effects of MTH and ADSCs on angiogenesis. Although treatment using MTH or ADSCs alone had only a marginal effect on the production of VEGF, the combination of MTH and ADSCs synergistically increased the levels of VEGF both in situ and in the periphery (**Figure 8**).

MTH in combination with ADSC administration effectively reduced the infiltration of innate immune cells during stroke

Innate immune cells respond to ischemic injury within hours. These infiltrating innate immune cells can be both beneficial and detrimental to the neural injury, which may largely depend on the local microenvironment. Studies have shown that MTH and ADSCs can regulate the balance of different types of immune responses to favor the resolution of neuroinflammation and neural regeneration (Leto et al., 2013; Talma et al., 2016). To investigate the effect of the combined MTH and ADSC therapy on neuroinflammation, we first compared the number of neutrophils (**Figure 9A** and **B**) and myeloid lineage cells (**Figure 9C** and **D**). MTH in combination with ADSCs strongly reduced the number of MPO$^+$ neutrophils and Iba1$^+$ myeloid lineage cells compared with single treatments. In keeping with that, we also found that pro-inflammatory cytokines such as interleukin (IL)-1 beta, tumor necrosis factor (TNF)-α, and IL-6 also decreased following the combination therapy (**Figure 9E–G**). Ym-1, an important marker that may be involved in neural regeneration, was strongly increased in the MTH $^+$ ADSC group (**Figure 9H**). Overall, these data suggested that the combined therapy of MTH and ADSCs shifted the balance of the innate immune response, providing a permissive environment that allowed neural regeneration.

Discussion

This study explored the possibility of combining MTH and MSC-based therapy for treating acute stroke, using a rodent tMCAO model. The combination of MTH and ADSCs substantially improved the neurological deficits and decreased the infarct size compared with application of MTH or ADSCs alone. In addition, we found that MTH and ADSC treatment synergistically reduced ischemia-induced neuronal loss. These beneficial effects of the combination therapy were associated with the down-regulation of innate inflammatory responses after stroke.

It has been suggested that ADSCs rescue neurons from ischemia-induced cell death through soluble factors (Gao et al., 2012). These soluble factors include neurotrophic factors that can promote neural cell regeneration (Salgado et al., 2010), and cytokines that can dampen inflammatory responses (Nauta and Fibbe, 2007; Ohtaki et al., 2008). These effects are a so-called "bystander" mechanism, whereby factors secreted from ADSCs promote functional recovery by protecting against inflammatory damage (Jeon et al., 2011, 2013), and only small proportion of ADSCs differentiate into neurons (Oh et al., 2015). Our *in vitro* results

suggested that ADSC supernatant acted as an effector to reduce cell damage or death; however, the protective effect was more obvious at 33°C. This suggested that hypothermia may increase the responsiveness of ischemic neurons to ADSC-based treatment. Future experiments are needed to explore the potential molecular mechanisms underlying this effect of hypothermia on ischemic neurons.

Various types of injury, including ischemia in the central nervous system, can lead to the activation and proliferation of astrocytes (Sofroniew et al., 2005). As part of the wound-healing process, the over-proliferation of astrocytes surrounding the lesion eventually forms a scar-like structure called the glial scar. The glial scar limits the amplification of the injury; however, growth-inhibitory molecules expressed by these astrocytes also prevent the migration of neural stem cells to the lesion and therefore impede neural regeneration. In our study, the combination therapy of MTH and ADSCs effectively reduced the number of GFAP$^+$ astrocytes. We postulate that the combination of MTH and ADSCs may inhibit the formation of the glial scar, which in turn enhances neural regeneration.

The blood-brain barrier is an important structure to maintain homeostasis of the central nervous system, and is composed of endothelial cells, pericytes, astrocytes, neurons, and extracellular matrix. The integrity of the blood-brain barrier can directly affect the prognosis of stroke models (Terasaki et al., 2014; Wang et al., 2014). Angiogenesis therefore plays a crucial role in neural repair at later time points after stroke. In our study, the expression of the angiogenesis marker, VEGF, was strongly upregulated after combined MTH and ADSC therapy compared with other groups. This may explain the long-term effect of the combination therapy that we observed on day 7.

During stroke, the ischemic insult triggers a cascade of immune reactions. As the first line of defense, innate immune cells such as neutrophils and myeloid lineage cells (macrophages and monocyte-derived macrophages) respond to ischemic brain injury within hours (Herz et al., 2015). The consequences of the immune response during stroke are complicated. On one hand, it prevents infection, and certain types (type II) of immune responses facilitate neural cell regeneration. On the other hand, over-production of inflammatory mediators such as pro-inflammatory cytokines may cause secondary injury to neural cells. MTH can down-regulate pro-inflammatory cytokine production, such as IL-6, by innate immune cells in humans (Aibiki et al., 1999). It is still not clear how MTH down-regulates immune responses. In addition, mesenchymal stem cells can also inhibit the production of multiple pro-inflammatory cytokines from innate immune cells through various molecules, including transforming growth factor-β, prostaglandin E2, indoleamine 2, 3-two-plus oxygen and TNFα-stimulated gene-6 (Hegyi et al., 2012; Lee et al., 2014; Xu et al., 2014). In the present study, the combination therapy showed a strong immunosuppressive effect, suggesting that MTH and ADSC treatment synergistically inhibits innate immune responses during stroke. Ym1, a functional marker of type II

innate immune cells (M2 and N2) was strongly increased by the combination therapy, indicating that the combination therapy may also be good at promoting tissue repair and the resolution of hyper-immune responses during stroke.

In summary, the combination of MTH and ADSC treatment is a safe and effective therapeutic approach for treating acute stroke and provides a rationale for further clinical application.

References

Aibiki M, Maekawa S, Ogura S, Kinoshita Y, Kawai N, Yokono S (1999) Effect of moderate hypothermia on systemic and internal jugular plasma IL-6 levels after traumatic brain injury in humans. J Neurotrauma 16:225-232.

Bacigaluppi M, Pluchino S, Martino G, Kilic E, Hermann DM (2008) Neural stem/precursor cells for the treatment of ischemic stroke. J Neurol Sci 265:73-77.

Chen J, Li Y, Wang L, Lu M, Zhang X, Chopp M (2001) Therapeutic benefit of intracerebral transplantation of bone marrow stromal cells after cerebral ischemia in rats. J Neurol Sci 89:49-57.

Chen J, Sanberg PR, Li Y, Wang L, Lu M, Willing AE, Sanchez-Ramos J, Chopp M (2001) Intravenous administration of human umbilical cord blood reduces behavioral deficits after stroke in rats. Stroke 32:2682-2688.

Chen J, Zhang C, Jiang H, Li Y, Zhang L, Robin A, Katakowski M, Lu M, Chopp M (2005) Atorvastatin induction of VEGF and BDNF promotes brain plasticity after stroke in mice. J Cereb Blood Flow Metab 25:281-290.
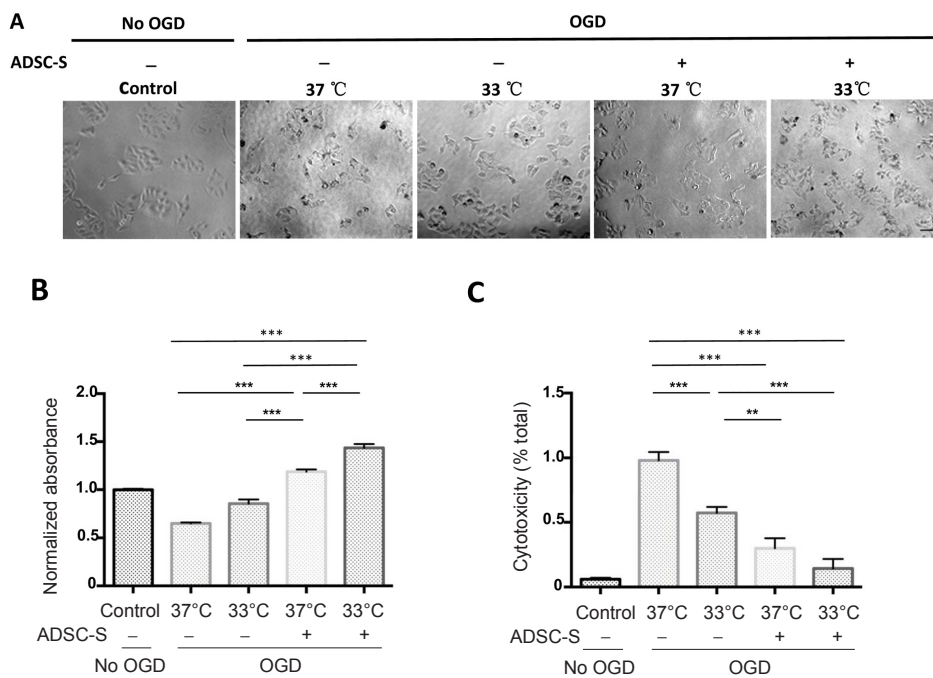
Figure 6 MTH increased the responsiveness of ischemic neurons to ADSC treatment *in vitro*.
SH-SY5Y cells were cultured under OGD condition for 24 hours at either the normal 37°C or at 33°C. ADSC-S was added to the cells. The morphology of the cells was observed by a light microscope (A). Relative cell viability and death were determined by MTT (B) and LDH assays (C), respectively. SH-SY5Y cells treated with mild hypothermia and ADSC-S showed increased viability and cytotoxicity compared with single treatments. All in vitro ischemic experiments were conducted in triplicate. Scale bars: 100 μm. Results are presented as the mean ± SEM (*n* = 6 per group; one-way analysis of variance followed by a Tukey's *post hoc* analysis); *$P < 0.05$, **$P < 0.01$, ***$P < 0.001$. MTH: Mild therapeutic hypothermia; ADSC: adipose-derived stem cell; ADSC-S: ADSC-supernatant; OGD: oxygen-glucose deprivation; MTT: 3-(4,5-dimethylthiazol-2-yl)-2,5-diphenyl tetrazolium bromide; LDH: lactate dehydrogenase.
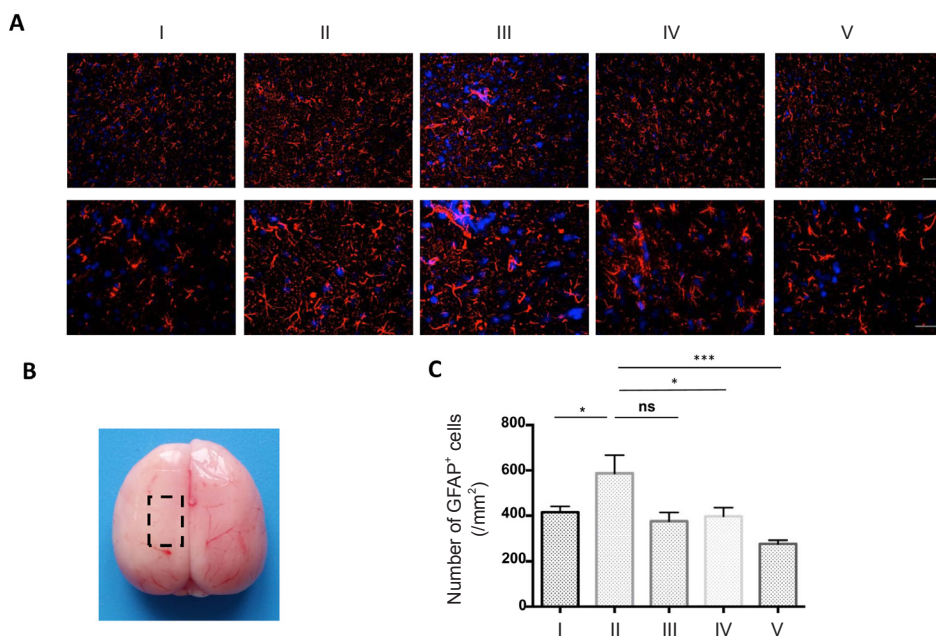

Figure 7 MTH in combination with ADSC administration reduced astrogliosis.
(A) GFAP immunofluorescence staining was used to identify the number of astrocytes. Scale bars: 100 μm. MTH in combination with ADSC administration dramatically reduced the number of GFAP-positive cells on day 1 (original magnification: upper, 20×; lower, 40×). (B) Each slice was taken from the region of the rat brain shown in the dotted box. (C) Counts of GFAP⁺ cells. Results are presented as the mean ± SEM (*n* = 6 per group; one-way analysis of variance followed by a Tukey's *post hoc* analysis); *$P < 0.05$, ***$P < 0.001$. I: Sham group; II: vehicle group (MCAO + PBS); III: ADSC group (MCAO + ADSC); IV: MTH group (MCAO + MTH); V: MTH + ADSC group (MCAO + MTH + ADSC). MTH: mild therapeutic hypothermia; ADSC: adipose-derived stem cell; GFAP: glial fibrillary acidic protein; ns: not significant.

Chi K, Fu RH, Huang YC, Chen SY, Lin SZ, Huang PC, Lin PC, Chang FK, Liu SP (2016) Therapeutic effect of ligustilide-stimulated adipose-derived stem cells in a mouse thromboembolic stroke model. Cell Transplant 259:899-912.

Chiang T, Messing RO, Chou WH (2011) Mouse model of middle cerebral artery occlusion. J Vis Exp 48:e2761.

Dai HB, Xu MM, Lv J, Ji XJ, Zhu SH, Ma RM, Miao XL, Duan ML (2016) Mild hypothermia combined with hydrogen sulfide treatment during resuscitation reduces hippocampal neuron apoptosis via NR2A, NR2B, and PI3K-Akt signaling in a rat model of cerebral ischemia-reperfusion injury. Mol Neurobiol 53:4865-4873.

Erecinska M, Thoresen M, Silver IA (2003) Effects of hypothermia on energy metabolism in Mammalian central nervous system. J Cereb Blood Flow Metab 23:513-530.

Feigin V, Anderson N, Gunn A, Rodgers A, Anderson C (2003) The emerging role of therapeutic hypothermia in acute stroke. Lancet Neurol 2:529-529.

Fisher M, Saver JL (2015) Future directions of acute ischaemic stroke therapy. Lancet Neurol 14:758-767.

Gao S, Zhao P, Lin C, Sun Y, Wang Y, Zhou Z, Yang D, Wang X, Xu H, Zhou F, Cao L, Zhou W, Ning K, Chen X, Xu J (2014) Differentiation of human adipose-derived stem cells into neuron-like cells which are compatible with photocurable three-dimensional scaffolds. Tissue Eng Part A 20:1271-1284.

Gao X, Dong T, Li ZQ, Jiang W, Wei XZ, Cao P, Liang GB (2012) Survival of human adipose-derived mesenchymal stem cells transplanted via the tail vein in rat brain with cerebral ischemia. Zhongguo Zuzhi Gongcheng Yanjiu 16:5067-5071.

Gutiérrez-Fernández M, Rodríguez-Frutos B, Álvarez-Grech J, Vallejo-Cremades MT, Expósito-Alcaide M, Merino J, Roda JM, Díez-Tejedor E (2011) Functional recovery after hematic administration of allogenic mesenchymal stem cells in acute ischemic stroke in rats. Neuroscience 175:394-405.
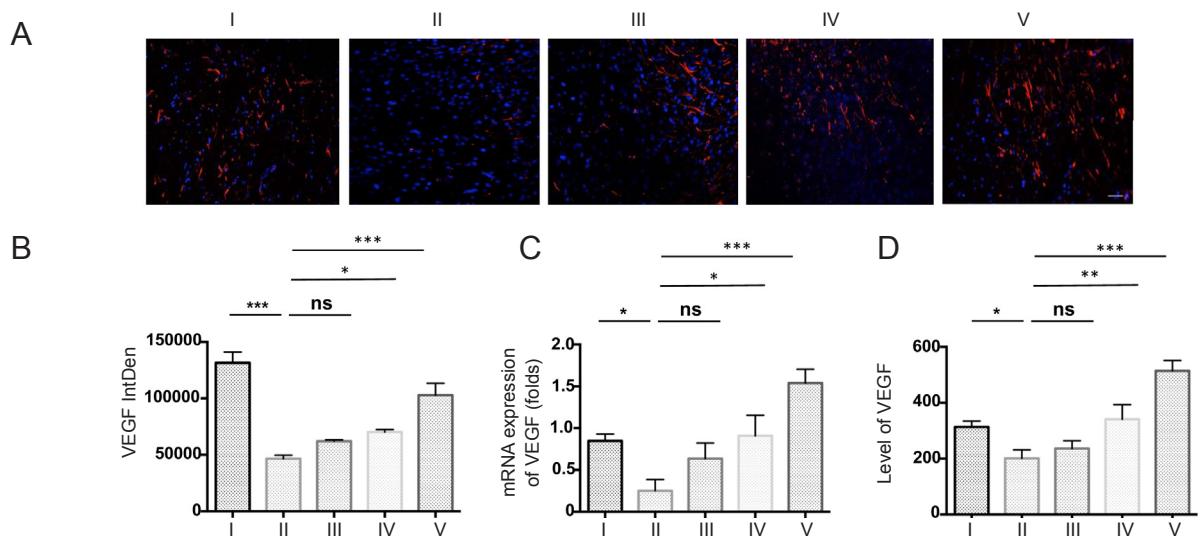
Figure 8 MTH in combination with ADSC administration increased VEGF expression.
(A) Immunofluorescence staining for VEGF in the ischemic lesion; (B) fluorescence intensity of VEGF; (C) real-time reverse transcription-polymerase chain reaction for VEGF mRNA; (D) enzyme linked immunosorbent assay for serum levels of VEGF. MTH combined with ADSCs strongly increased VEGF expression both *in situ* and in the periphery compared with other groups. Results are presented as the mean ± SEM (n = 6 per group; one-way analysis of variance followed by a Tukey's *post hoc* analysis); *P < 0.05, **P < 0.01, ***P < 0.001.I: Sham group; II: vehicle group (MCAO + PBS); III: ADSC group (MCAO + ADSC); IV: MTH group (MCAO + MTH); V: MTH + ADSC group (MCAO + MTH + ADSC). MTH: mild therapeutic hypothermia; ADSC: adipose-derived stem cell; VEGF: vascular endothelial growth factor; ns: not significant.
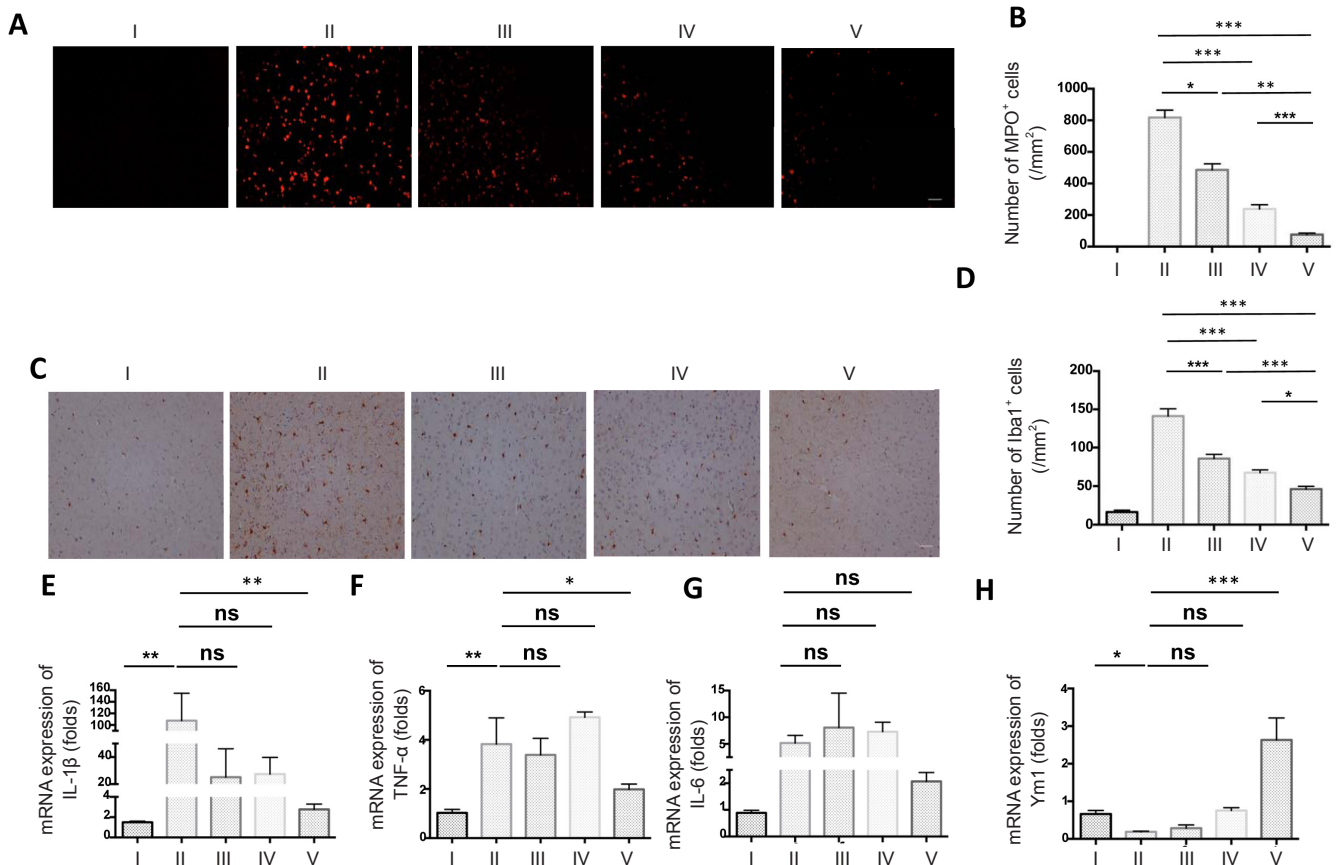

Figure 9 MTH in combination with ADSC administration effectively reduced the infiltration of innate immune cells during stroke.
(A) Images of MPO in the ischemic core of the cerebral cortex; (B) counts of MPO-positive cells; (C) images of Iba1 in the ischemic core of the cerebral cortex; (D) counts of Iba1-positive cells. Scale bars: 100 μm. Both the number of MPO-positive cells and the counts of Iba1+ myeloid lineage cells were reduced in group V to a greater extent than in the other treatment groups on day 1 after transient middle cerebral artery occlusion. The expression of pro-inflammatory cytokine IL-1β (E), TNF-α (F), and IL-6 (G), and Ym1 (H) were measured by real-time reverse transcription-polymerase chain reaction. Results are presented as the mean ± SEM (n = 6 per group; one-way analysis of variance followed by a Tukey's *post hoc* analysis); *P < 0.05, **P < 0.01, ***P < 0.001. I: Sham group; II: vehicle group (MCAO + PBS); III: ADSC group (MCAO + ADSC); IV: MTH group (MCAO + MTH); V: MTH + ADSC group (MCAO + MTH + ADSC). MTH: mild therapeutic hypothermia; ADSC: adipose-derived stem cell; MPO: myeloperoxidase; IL: interleukin; TNF-α: tumor necrosis factor α; Ym1: chitinase 3-like 3; ns: not significant.

Gutiérrez-Fernández M, Rodríguez-Frutos B, Ramos-Cejudo J, Otero-Ortega L, Fuentes B, Vallejo-Cremades MT, Sanz-Cuesta BE, Díez-Tejedor E (2015) Comparison between xenogeneic and allogeneic adipose mesenchymal stem cells in the treatment of acute cerebral infarct: proof of concept in rats. J Transl Med 13:46.

Hankey GJ (2013) The global and regional burden of stroke. Lancet Glob 1:239-240.

Hao L, Zou Z, Tian H, Zhang Y, Zhou H, Liu L (2014) Stem cell-based therapies for ischemic stroke. Biomed Res 2014:468748.

Hegyi B, Kudlik G, Monostori E, Uher F (2012) Activated T-cells and pro-inflammatory cytokines differentially regulate prostaglandin E2 secretion by mesenchymal stem cells. Biochem Biophys Res Commun 419:215-220.

Herz J, Sabellek P, Lane TE, Gunzer M, Hermann DM, Doeppner TR (2015) Role of neutrophils in exacerbation of brain injury after focal cerebral ischemia in Hyperlipidemic Mice. Stroke 46:2916-2925.

Jeon D, Chu K, Lee ST, Jung KH, Ban JJ, Park DK, Yoon HJ, Jung S, Yang H, Kim BS, Choi JY, Kim SH, Kim JM, Won CH, Kim M, Lee SK, Roh JK (2013) Neuroprotective effect of a cell-free extract derived from human adipose stem cells in experimental stroke models. Neurobiol Dis 54:414-420.

Jeon D, Chu K, Lee ST, Jung KH, Kang KM, Ban JJ, Kim S, Seo JS, Won CH, Kim M, Lee SK, Roh JK (2011) A cell-free extract from human adipose stem cells protects mice against epilepsy. Epilepsia 52:1617-1626.

Jin K, Sun Y, Xie L, Mao XO, Childs J, Peel A, Logvinova A, Banwait S, Greenberg DA (2005) Comparison of ischemia-directed migration of neural precursor cells after intrastriatal, intraventricular, or intravenous transplantation in the rat. Neurobiol Dis 18:366-374.

Kammersgaard LP, Jørgensen HS, Rungby JA, Reith J, Nakayama H, Weber UJ, Houth J, Olsen TS (2002) Admission body temperature predicts long-term mortality after acute stroke: the Copenhagen Stroke Study. Stroke 33:1759-1762.

Karibe H, Zarow GJ, Graham SH Weinstein PR (1994) Mild intraischemic hypothermia reduces postischemic hyperperfusion, delayed postischemic hypoperfusion, blood-brain barrier disruption, brain edema, and neuronal damage volume after temporary focal cerebral ischemia in rats. J Cereb Blood Flow Metab 14:620-627.

Lee JH, Wei L, Gu X, Won S, Wei ZZ, Dix TA, Yu SP (2016) Improved therapeutic benefits by combining physical cooling with pharmacological hypothermia after severe stroke in rats. Stroke 47:1907-1913.

Lee RH, Yu JM, Foskett AM, Peltier G, Reneau JC, Bazhanov N, Oh JY, Prockop DJ (2014) TSG-6 as a biomarker to predict efficacy of human mesenchymal stem/progenitor cells (hMSCs) in modulating sterile inflammation in vivo. PNAS 111:16766-16771.

Lee SK, Kim M, Roh JK (2009) Slowed progression in models of Huntington disease by adipose stem cell transplantation. Ann Neurol 66:671-681.

Lee ST, Chu K, Jung KH, Kim SJ, Kim DH, Kang KM, Hong NH, Kim JH, Ban JJ, Park HK, Kim SU, Park CG, Lee SK, Kim M, Roh JK (2008) Anti-inflammatory mechanism of intravascular neural stem cell transplantation in haemorrhagic stroke. Brain 131:616-629.

Leto Barone AA, Khalifian S, Lee WP, Brandacher G (2013) Immunomodulatory effects of adipose-derived stem cells: fact or fiction? Biomed Res Int 2013:383685.

Leu S, Lin YC, Yuen CM, Yen CH, Kao YH, Sun CK, Yip HK (2010) Adipose-derived mesenchymal stem cells markedly attenuate brain infarct size and improve neurological function in rats. J Transl Med 8:63.

Li D, Fang Y, Wang P, Shan W, Zuo Z, Xie L (2012) Autologous transplantation of adipose-derived mesenchymal stem cells attenuates cerebral ischemia and reperfusion injury through suppressing apoptosis and inducible nitric oxide synthase. Int J Mol Med 29:848-854.

Li Y, Chopp M (2009) Marrow stromal cell transplantation in stroke and traumatic brain injury. Neurosci Lett 456:120-123.

Li Y, Chopp M, Chen J, Wang L, Gautam SC, Xu YX, Zhang Z (2000) Intrastriatal transplantation of bone marrow nonhematopoietic cells improves functional recovery after stroke in adult mice. J Cereb Blood Flow Metab 20:1311-1319.

Longa EZ, Weinstein PR, Carlson S, Cummins R (1989) Reversible middle cerebral artery occlusion without craniectomy in rats. stroke 20:84-91.

Nam HS, Kwon I, Lee BH, Kim H, Kim J, An S, Lee OH, Lee PH, Kim HO, Namgoong H, Kim YD, Heo JH (2015) Effects of mesenchymal stem cell treatment on the expression of matrix metalloproteinases and angiogenesis during ischemic stroke recovery. PLoS One 10:e0144218.

Nauta AJ, Fibbe WB (2007) Immunomodulatory properties of mesenchymal stromal cells. Blood 110:3499-3506.

Oh SH, Choi C, Chang DJ, Shin DA, Lee N, Jeon I, Sung JH, Lee H, Hong KS, Ko JJ, Song J (2015) Early neuroprotective effect with lack of long-term cell replacement effect on experimental stroke after intra-arterial transplantation of adipose-derived mesenchymal stromal cells. Cytotherapy 17:1090-1103.

Ohtaki H, Ylostalo JH, Foraker JE, Robinson AP, Reger RL, Shioda S, Prockop DJ (2008) Stem/progenitor cells from bone marrow decrease neuronal death in global ischemia by modulation of inflammatory/immune responses Proc Natl Acad Sci U S A 105:14638-14643.

Puissant B, Barreau C, Bourin P, Clavel C, Corre J, Bousquet C, Taureau C, Cousin B, Abbal M, Laharrague P, Penicaud L, Casteilla L, Blancher A (2005) Immunomodulatory effect of human adipose tissue-derived adult stem cells: comparison with bone marrow mesenchymal stem cells. Br J Haematol 129:118-129.

Safford KM, Safford SD, Gimble JM, Shetty AK, Rice HE (2004) Characterization of neuronal/glial differentiation of murine adipose-derived adult stromal cells. Experimental Neurology 187: 319-328.

Salgado AJ, Reis RL, Sousa NJ, Gimble JM (2010) Adipose tissue derived stem cells secretome: soluble factors and their roles in regenerative medicine. Cur Stem Cell Res Ther 5:103-110.

Shen LH, Li Y, Chen J, Zhang J, Vanguri P, Borneman J, Chopp M (2006) Intracarotid transplantation of bone marrow stromal cells increases axon-myelin remodeling after stroke. Neuroscience 137:393-399.

Sofroniew MV (2005) Reactive astrocytes in neural repair and protection. Neuroscientist 11:400-407.

Talma N, Kok WF, de Veij Mestdagh CF, Shanbhag NC Bouma HR, Henning RH (2016) Neuroprotective hypothermia-Why keep your head cool during ischemia and reperfusion. Biochim Biophys Acta 1860:2521-2528.

Terasaki Y, Liu Y, Hayakawa K, Pham LD, Lo EH, Ji X, Arai K (2014) Mechanisms of neurovascular dysfunction in acute ischemic brain. Curr Med Chem 21:2035-2042.

Tobita M, Orbay H, Mizuno H (2011) Adipose-derived stem cells: current findings and future perspectives. Discov Med 11:160-170.

Wang L, Jiang F, Li Q, He X, Ma J (2014) Mild hypothermia combined with neural stem cell transplantation for hypoxic-ischemic encephalopathy: neuroprotective effects of combined therapy. Neural Regen Res 9:1745-1752.

Wang X, Zhang M, Feng R, Li WB, Ren SQ, Zhang J, Zhang F (2014) Physical exercise training and neurovascular unit in ischemic stroke. Neuroscience 271:99-107.

Xu C, Yu P, Han X, Du L, Gan J, Wang Y, Shi Y (2014) TGF-beta promotes immune responses in the presence of mesenchymal stem cells. J Immunol 192:103-109.

Yenari MA, Han MH (2012) Neuroprotective mechanisms of hypothermia in brain ischaemia. Nat Rev Neurosci 13:267-278.

Yu GL, Liang Y, Huang ZM, Jones DW, Pritchard KA Jr, Zhang G (2016) Inhibition of myeloperoxidase oxidant production by N-acetyl lysyltyrosylcysteine amide reduces brain damage in a murine model of stroke. J Neuroinflamm 13:119-131.

Zeng GF, Lai K, Li J, Zou YQ, Huang HL, Liang J, Tang XD, Wei J, Zhang PH (2013) A rapid and efficient method for primary culture of human adipose-derived stem cells. Organogenesis 9:287-295.

Zhao H, Steinberg GK, Sapolsky RM (2007) General versus specific actions of mild-moderate hypothermia in attenuating cerebral ischemic damage. J Cereb Blood Flow Metab 27:1879-1894.

Zhao K, Li R, Gu CC, Liu L, Jia YL, Guo XZ, Zhang WP, Pei CY, Tian LL, Li B, Jia JR, Cheng HK, Xu HW, Li LX (2017) Intravenous administration of Adipose-derived stem cell (ADSC) protein extracts improves neurological deficits in a rat model of stroke. Stem Cells Int 2017:2153629.

Zuk PA, Zhu M, Mizuno H, Huang J, Futrell JW, Katz AJ, Benhaim P, Lorenz HP, Hedrick MH (2001) Multilineage cells from human adipose tissue: implications for cell-based therapies. Tissue Eng 7:211-228.

(Copyedited by Turnley A, Raye W, Wang J, Li CH, Qiu Y, Song LP, Zhao M)